PLASTIC DAMAGE MODEL FOR PROGRESSIVE FAILURE ANALYSIS OF COMPOSITE STRUCTURES

J. F. Chen, E. V. Morozov*, K. Shankar
School of Engineering and Information Technology, University of New South Wales at the Australian Defence Force Academy, Canberra, Australia
* Corresponding author (e.morozov@adfa.edu.au)

Keywords: *plastic damage model, progressive failure analysis, composite structures, return mapping algorithm*

1 Introduction

Laminated composite materials are widely used in aerospace, civil, shipbuilding and other industries due to their high strength and stiffness to weight ratios, good fatigue resistance and high energy absorption capacity. In many structural applications, the progressive failure analysis is required to predict their mechanical response under various loading conditions.

The use of appropriate material constitutive models plays a crucial role in progressive failure analysis of composite structures. Most of the damage mechanics based composite material models fall into the elastic-damage category [1-6]. In these models, irreversible deformations are not normally considered in the unloading stage. Although this might be suitable for modelling the mechanical behaviour of elastic-brittle composites, experimental studies [7,8] show that some thermoset or thermoplastic composites exhibit apparent plastic response, especially under transverse and/or shear stresses. Numerical investigation also reveals that the model that does not take into account the plastic nature of composites might be insufficient, in some instances, in the evaluation of energy absorption capacity of composite structures [9]. In addition, damage accumulated within the plies could lead to the material properties degradation before the collapse of the composite structures. The consideration of material properties degradation improves the predictions of failure loads [10].

This paper attempts to develop a combined plastic damage model for composites, which accounts for both the plasticity effects and material properties degradation of composite materials under loading. The plasticity effects are modelled using the approach proposed by Sun and Chen [11]. The prediction of the damage initiation and propagation in the laminated composites takes into account various failure mechanisms employing Hashin's failure criteria [12].

The proposed plastic damage model is implemented in Abaqus/Standard using a user-defined subroutine (UMAT). The strain-driven implicit integration procedure for the proposed model is developed using equations of continuum damage mechanics, plasticity theory and applying the return mapping algorithm. To ensure the algorithmic efficiency of the Newton-Raphson method in the finite element analysis, a tangent operator that is consistent with the developed integration algorithm is formulated. The efficiency of the proposed model is verified by performing progressive failure analysis of composite laminates containing central hole and subjected to in-plane tensile loads. The predicted results agree well with the test data and provide accurate estimates of the failure loads.

2 Plastic damage constitutive model

2.1 Stress-strain relationship

The proposed plastic damage model is formulated for an elementary orthotropic ply and describes both the plastic response and the damage development which is based on the stiffness reduction approach.

The damage effects are taken into account by introducing damage variables in the stiffness matrix using the continuum damage mechanics concept. The stress-strain relationships for the damaged and undamaged composite materials are written as follows:

$$\bar{\boldsymbol{\sigma}} = \mathbf{S_0} : \boldsymbol{\varepsilon}^e = \mathbf{S_0} : (\boldsymbol{\varepsilon} - \boldsymbol{\varepsilon}^p); \qquad (1)$$
$$\boldsymbol{\sigma} = \mathbf{S}(d) : \boldsymbol{\varepsilon}^e = \mathbf{S}(d) : \left(\boldsymbol{\varepsilon} - \boldsymbol{\varepsilon}^p\right)$$

where bold-face symbols are used for variables of tensorial character and symbol (**:**) denotes inner product of two tensors with double contraction, e.g. $((\mathbf{S}(d) : \boldsymbol{\varepsilon}^e)_{ij}) = \mathrm{S}(d)_{ijkl}\varepsilon_{kl}{}^e$, where the summation convention is applied to the subscripts; $\boldsymbol{\sigma}$, $\bar{\boldsymbol{\sigma}}$ are the Cauchy stress tensor and the effective stress tensor (both are the second order tensors); $\mathbf{S}_0$ is the fourth-order constitutive tensor for linear-elastic undamaged unidirectional laminated composites; $\mathbf{S}(d)$ is the one for the corresponding damaged materials; $\boldsymbol{\varepsilon}$, $\boldsymbol{\varepsilon}^e$, $\boldsymbol{\varepsilon}^p$ are the total strain, elastic strain, and plastic strain tensors, respectively; d is the damage variable. The form of the $\mathbf{S}(d)$ adopted in this model is similar to that presented by Matzenmiller et al. [2]

$$\mathbf{S}(d) = \frac{1}{D}\begin{bmatrix} (1-d_1)E_1^0 & Bv_{21}^0E_1^0 & 0 \\ Bv_{12}^0E_1^0 & (1-d_2)E_2^0 & 0 \\ 0 & 0 & D(1-d_3)G_{12}^0 \end{bmatrix} \quad (2)$$

where $D = 1-(1-d_1)(1-d_2)v_{12}^0v_{21}^0$; parameter $B = (1-d_1)(1-d_2)$; parameters d_1, d_2, d_3 denote damage developed in the fibre and transverse direction, and under shear (theses damage variables are constant throughout the ply thickness); E_1^0, E_2^0, G_{12}^0 and v_{12}^0, v_{21}^0 are elastic moduli and Poisson's ratios of undamaged unidirectional composite laminae.

In order to differentiate between the effects of compression and tension on the failure modes, the damage variables are presented as follows:

$$d_1 = \begin{cases} d_{1t} & \text{if } \sigma_1 \geq 0 \\ d_{1c} & \text{if } \sigma_1 < 0 \end{cases} \qquad d_2 = \begin{cases} d_{2t} & \text{if } \sigma_2 \geq 0 \\ d_{2c} & \text{if } \sigma_2 < 0 \end{cases} \quad (3)$$

where d_{1t}, d_{1c} characterise the damage development caused by tension and compression in the fibre direction, and d_{2t}, d_{2c} reflect the damage development caused by tension and compression in the transverse direction. It is assumed that the shear stiffness reduction results from the fibre and matrix cracking. To take this into account, the corresponding damage variable d_3 is expressed as:

$$d_3 = 1-(1-d_6)(1-d_{1t}) \quad (4)$$

where d_6 represents the damage effects on shear stiffness caused by matrix cracking.

2.2 Plastic model

Plasticity is assumed to occur in the undamaged area of the composites. The plastic yield function is expressed in terms of effective stresses as follows:

$$F(\overline{\boldsymbol{\sigma}}, \tilde{\varepsilon}^p) = F^p(\overline{\boldsymbol{\sigma}}) - \kappa(\tilde{\varepsilon}^p) = 0 \quad (5)$$

where F^p is the plastic potential; κ is the hardening parameter which depends on the plastic deformations and is expressed in terms of equivalent plastic strain $\tilde{\varepsilon}^p$.

Due to its simplicity and accuracy, an equivalent form of the one-parameter plastic yield function for plane stress condition proposed by Sun and Chen [11] is adopted in this study:

$$F(\overline{\boldsymbol{\sigma}}, \tilde{\varepsilon}^p) = \sqrt{\frac{3}{2}\left(\bar{\sigma}_2^2 + 2a\,\bar{\sigma}_3^2\right)} - \tilde{\sigma}(\tilde{\varepsilon}^p) = 0 \quad (6)$$

where a is a material parameter which describes the level of plastic deformation developed under shear loading compared to the transverse loading; $\bar{\sigma}_2$ is the effective stress in the transverse direction, $\bar{\sigma}_3$ is the effective in-plane shear stress . Note that the use of this form of yield function improves efficiency and accuracy of the computational algorithm.

For the sake of simplicity, an isotropic hardening law expressed in terms of equivalent plastic strain $\tilde{\varepsilon}^p$ is adopted in this work. The following formulation of this law proposed by Sun and Chen [11] is used to represent the equivalent stress versus equivalent plastic strain hardening curve:

$$\kappa(\tilde{\varepsilon}^p) = \tilde{\sigma}(\tilde{\varepsilon}^p) = \beta(\tilde{\varepsilon}^p)^n \quad (7)$$

where $\tilde{\sigma}$ is the equivalent stress defined as follows:

$$\tilde{\sigma} = \left[\frac{3}{2}\,\bar{\sigma}_2^2 + 2a\,\bar{\sigma}_3^2\right]^{\frac{1}{2}} \quad (8)$$

In Eq.(7), β and n are coefficients that fit the experimental hardening curve. These parameters together with the material parameter a are determined using an approach based on the linear regression analysis of the results obtained from the off-axis tensile tests performed on the unidirectional composite specimens [11, 13].

The associated plastic flow rule is assumed for the plastic evolution in composites. According to this law, the plastic strain rate is expressed as:

$$\dot{\boldsymbol{\varepsilon}}^p = \dot{\lambda}^p \partial_{\bar{\sigma}} F \quad (9)$$

where $\dot{\lambda}^p \geq 0$ is a nonnegative plastic consistency parameter; hereafter $\partial_x y = \partial y / \partial x$.

Similarly, the associated equivalent plastic flow rule is also adopted in the following form:

$$\dot{\tilde{\varepsilon}}^p = \dot{\lambda}^p \partial_{\tilde{\varepsilon}^p} F \quad (10)$$

The equivalent plastic strain rate can be obtained from the equivalence of the rates of the plastic work per unit volume W^p:

$$\dot{W}^p = \overline{\boldsymbol{\sigma}} : \dot{\boldsymbol{\varepsilon}}^p = \tilde{\sigma}\,\dot{\tilde{\varepsilon}}^p \quad (11)$$

Making use of Eq. (6), and taking into account Eqs. (8) - (11), the following relation is derived:

$$\dot{\tilde{\varepsilon}}^p = \dot{\lambda}^p \quad (12)$$

2.3 Damage model

2.3.1 Damage initiation and propagation criteria

In order to predict the damage initiation and propagation of each intralaminar failure of the material and evaluate the effective stress state, the damage initiation and propagation criteria f_I are presented in the following form:

$$f(\phi_I, r_I) = \phi_I - r_I \leq 0 \tag{13}$$

$$I = \{1t, 1c, 2t, 2c, 6\}$$

where ϕ_I is the loading function adopted in the form of Hashin's failure criteria [12]; r_I is the damage threshold corresponding to each failure mechanism. The latter parameter r_I controls the size of the expanding damage surface and depends on the loading history. The initial damage threshold $r_{I,0}$ equals unity. As mentioned previously, the damage variable d_6 represents the damage effects on the shear stiffness due to matrix facture caused by a combined action of transverse and shear stresses. However, the compressive transverse stress has beneficial effects on the matrix cracking. Thus, it is reasonable to assume that the damage effects are governed by the tensile matrix cracking, i.e. $f_6 = f_{2t}$, $r_6 = r_{2t}$.
According to the Hashin's failure criteria, the loading functions for different failure mechanisms are given as follows:

$$\phi_{1t} = \left(\frac{\bar{\sigma}_1}{X_t}\right)^2 \quad (\bar{\sigma}_1 \geq 0) \tag{14}$$

$$\phi_{1c} = \left(\frac{\bar{\sigma}_1}{X_c}\right)^2 \quad (\bar{\sigma}_1 < 0) \tag{15}$$

$$\phi_{2t} = \left(\frac{\bar{\sigma}_2}{Y_t}\right)^2 + \left(\frac{\bar{\sigma}_3}{S_c}\right)^2 \quad (\bar{\sigma}_2 \geq 0) \tag{16}$$

$$\phi_{2c} = \left(\frac{\bar{\sigma}_2}{Y_c}\right)^2 + \left(\frac{\bar{\sigma}_3}{S_c}\right)^2 \quad (\bar{\sigma}_2 < 0) \tag{17}$$

where X_t, X_c are the tensile and compressive strengths in fibre direction; Y_t, Y_c are the transverse tensile and compressive strengths; S_c is the shear strength.

2.3.2 Damage evolution

Under damage loading (i.e. when Eq. (13) is converted to equality) the damage consistency condition $\dot{f}_I = \dot{\phi}_I - \dot{r}_I = 0$ is satisfied, then the following expressions for damage threshold r_I can be derived:

$$r_I = \max\{1, \max\{\phi_I^\tau\}\} \quad \tau \in [0, t] \tag{18}$$

Since damage is irreversible, the damage evolution rate should satisfy the following condition: $\dot{d} \geq 0$. The exponential damage evolution law is adopted for each damage variable and expressed in the following form [14]:

$$d_I = 1 - \frac{1}{r_I}\exp\left(A_I(1 - r_I)\right) \tag{19}$$

where A_I is determined by regularizing the softening branch of the stress-strain curve to ensure the computed damage energy within an element is constant and to maintain the mesh objectivity. The regularization is based on the Bazant's crack band theory [15]. According to this, the damage energy dissipated per unit volume g_I for uniaxial or shear stress condition is related to the critical strain energy release rate $G_{I,c}$ along with the characteristic length of the finite element l^*:

$$g_I = \frac{G_{I,c}}{l^*} \tag{20}$$

where the critical strain energy release rates $G_{2t,c}$, $G_{6,c}$ are referred to as the intralaminar mode I and mode II fracture toughness parameters. The parameter $G_{1c,c}$ is the intralaminar mode I fracture toughness under compression. The parameters $G_{1t,c}$, $G_{1c,c}$ are the mode I fracture toughness parameters related to fibre breakage under tension and compression. The identification of these parameters and the characteristic length l^* is discussed in [4, 16]. The damage energy dissipated per unit volume for uniaxial or shear stress condition is obtained from the integration of the damage energy dissipation during the process of development:

$$g_I(A_I) = \int_0^\infty Y_I \, \dot{d}_I(A_I) dt \tag{21}$$

$$Y_I = -\frac{\partial \psi}{\partial d_I}; \psi = \frac{1}{2}\sigma : \varepsilon$$

where Y_I is the damage energy release rate; $\dot{d}_I$ is the rate of damage development defined as $\dot{d}_I = \mathrm{d}d_I/\mathrm{d}t$, ψ is the Helmhotlz free energy. Equating Eq. (20) and Eq. (21), the parameter A_I is determined numerically using iterative root-finding procedure.

3 Numerical implementation

The proposed plastic damage material model has been embedded in Abaqus/Standard finite element software package using the user-defined subroutine UMAT. The numerical integration algorithms updating the Cauchy nominal stresses and solution-dependent state variables are derived as well as the tangent matrix that is consistent with the numerical integration algorithm ensuring the quadratic convergence rate of the Newton-Raphson method in the finite element analysis.

3.1 Integration algorithm

The solution of the nonlinear inelastic problem under consideration is based on the incremental approach and is regarded as strain driven. The loading history is discretized into a sequence of time steps $[t_n, t_{n+1}]$, $n \in \{0,1,2,3 \ldots\}$ where each step is referred to as the $(n+1)$th increment. Driven by the strain increment $\Delta\boldsymbol{\varepsilon}$, the discrete problem in the context of backward Euler scheme for the combined plastic damage model can be stated as: for a given variable set $\{\boldsymbol{\varepsilon}_{n+1},\ \boldsymbol{\varepsilon}_{\boldsymbol{n}}^{\boldsymbol{p}},\ \tilde{\varepsilon}_n^p,\ \overline{\boldsymbol{\sigma}}_n,\ \boldsymbol{\sigma}_n,\ \tilde{\sigma}_n,\ r_{I,n},\ d_{I,n}\}$ at the beginning of the $(n+1)$th increment, find the updated variable set $\{\boldsymbol{\varepsilon}_{n+1}^{\boldsymbol{p}},\ \tilde{\varepsilon}_{n+1}^p,\ \overline{\boldsymbol{\sigma}}_{n+1},\ \boldsymbol{\sigma}_{n+1},\ \tilde{\sigma}_{n+1},\ r_{I,n+1},\ d_{I,n+1}\}$ at the end of the $(n+1)$th increment. The updated stresses and solution-dependent state variables are stored at the end of the $(n+1)$th increment and are passed on to the user subroutine UMAT at the beginning of the next increment. The integration scheme consists of two parts, namely, updating the effective stresses and updating the nominal Cauchy stresses. The closest point return mapping algorithm employing the backward Euler integration procedure is applied for updating the effective stresses. Substituting the updated effective stresses into the damage model, the damage variables are updated. According to Eq. $(1)_2$, the Cauchy stresses are calculated as follows:

$$\boldsymbol{\sigma}_{n+1} = \mathbf{S}(d_{n+1}) : \boldsymbol{\varepsilon}_{n+1}^e \tag{22}$$

3.2 Consistent tangent matrix

The consistent tangent matrix for the proposed combined plastic damage model is derived as follows:

$$\frac{\mathrm{d}\boldsymbol{\sigma}_{n+1}}{\mathrm{d}\boldsymbol{\varepsilon}_{n+1}} = [M_{n+1} + \mathbf{S}(d_{n+1})] : \mathbf{C}_0 : \mathbf{S}_{\mathrm{n+1}}^{\mathrm{alg}} \tag{23}$$

in which M_{n+1} is expressed in the indicial form as follows:

$$M_{ik}|_{n+1} = \varepsilon_j{}^e \frac{\partial \mathrm{S}(d)_{ij}}{\partial \varepsilon^e d_p} \frac{\partial d_p}{\partial r_t} \frac{\partial r_t}{\partial \phi_t} \frac{\partial \phi_t}{\partial \bar{\sigma}_q} \frac{\partial \bar{\sigma}_q}{\partial \varepsilon_k^e}\Bigg|_{n+1}$$

$$p, q, k = \{1, 2, 3\};\ t = \{1, 2\}$$

where matrix M_{ik} is of asymmetric. This results in the asymmetry of the consistent tangent matrix of the elastoplastic damage model. In Eq.(23), $\mathbf{C}_0 = \mathbf{S}_0^{-1}$ is the fourth-order compliance tensor for undamaged unidirectional laminated composite materials and $\mathbf{S}_{\mathrm{n+1}}^{\mathrm{alg}}$ is the consistent tangent matrix for plastic problem Eq. (6). The latter is expressed as:

$$\mathbf{S}_{\mathrm{n+1}}^{\mathrm{alg}} = \tilde{\mathbf{S}}_{n+1} - \frac{(\tilde{\mathbf{S}}_{n+1}:\partial_{\bar{\sigma}} F_{n+1}^p)\otimes(\tilde{\mathbf{S}}_{n+1}:\partial_{\bar{\sigma}} F_{n+1})}{\partial_{\bar{\sigma}} F_{n+1}:\tilde{\mathbf{S}}_{n+1}:\partial_{\bar{\sigma}} F_{n+1}^p - \partial_{\tilde{\varepsilon}^p} F_{n+1}} \tag{24}$$

where $\tilde{\mathbf{S}}_{n+1} = \left(\mathbf{C}_0 + \Delta\lambda_{\mathrm{n+1}}^{\mathrm{p}}\, \partial_{\bar{\boldsymbol{\sigma}}\bar{\boldsymbol{\sigma}}} \mathrm{F}_{\mathrm{n+1}}^{\mathrm{p}}\right)^{-1}$, $\Delta\lambda_{\mathrm{n+1}}^{\mathrm{p}}$ denotes the increment of λ^p in the (n+1)th increment; $\partial_{xx} y = \partial^2 y/\partial x^2$, and $(\otimes)$ denotes a tensor product. As the time increment Δt approaches zero, the increment of the plastic consistency parameter $\Delta\lambda_{n+1}^p$ approaches zero. Thus, $\tilde{\mathbf{S}}_{n+1}$ approaches $\mathbf{S}_0$, and $\mathbf{S}_{\mathrm{n+1}}^{\mathrm{alg}}$ reduces to the elastoplastic tangent operator when standard procedures of classical plasticity theory are applied.

3.3 Viscous regularization

Numerical simulations based on the implicit procedures, such as Abaqus/Standard, and the use of material constitutive models that are considering strain softening and material stiffness degradation often abort prematurely due to convergence problems. In order to alleviate these computational difficulties and improve convergence, a viscous regularization scheme has been implemented in the following form [5]:

$$\dot{d}_m^v = \frac{1}{\eta}(d_m - d_m^v), \quad m = \{1, 2,3\} \tag{25}$$

where d_m is the damage variable obtained as described previously, d_m^v is the regularized viscous damage variable, and η is the viscosity coefficient.
The corresponding regularized consistent tangent matrix is derived as:

$$\left.\frac{d\sigma_{n+1}}{d\varepsilon_{n+1}}\right|_v = [M_{n+1}^v + S(d_{n+1}^v)] : C_0 : S_{n+1}^{\mathrm{alg}}; \tag{26}$$

$$M_{n+1}^v = M(d_{n+1}^v) \cdot \frac{\Delta t}{\eta + \Delta t}$$

4 Numerical Results and Verifications

The proposed plastic damage model is applied to the progressive failure analyses of a set of AS4/PEEK $[0/45/90/\text{-}45]_{2s}$ laminates containing a through hole. The hole diameters are ranging from 2 to 10 mm. The laminates are subjected to in-plane tensile loading. The length, width and thickness of the laminates are 100 mm, 20 mm, and 2 mm, respectively. The material elastic properties and plastic model parameters are obtained from Sun and Yoon [17]. The compressive strengths are adopted from Sun and Rui [18], while the tensile strengths and shear strength are obtained from Kawai et al. [19]. The critical strain energies $G_{1t,c}$ and $G_{2t,c}$ are measured by Carlile [20]. The value of parameter $G_{6,c}$ is taking from [21]. The parameter $G_{2c,c}$ is calculated using $G_{6,c}$ and the equation suggested in Maimi [4]. The material constants and model parameters are listed in Table 1. The predicted failure loads were compared with the experimental data reported in Maa and Cheng [10] and their predictions based on the principal damage model and the modified principal damage model (referred to as Model 1 and Model 2 in this work). As shown in Table 2, the predicted results agree well with the test data. It follows from Table 2 that the results predicted using the model developed in this work are more accurate than those obtained using the model 1 model and have similar accuracy as those obtained from Model 2. The load versus displacement curves predicted using the present constitutive model are shown in Figure 1. The preditced damage evolution of the ply reinfroced at 0° within the laminate with the hole diameter of 5 mm characterized by the damage variables d_1, d_2, d_6, d_3 at the failure load and at the end of the analysis (labeled A and B in Figure 1) is presented in Figure 2.

5 Conclusions

A plastic damage constitutive model has been developed for the progressive failure analysis of composite laminates. This model takes into account both the plasticity effects and the material properties degradations exhibitied by composite materials. The corresponding strain-driven implicit integration algorithm based on the closest point return mappling algorithm has been developed as well as the tangent operator that is consistent with the derived integration algorithm. The material model has been verified by performing progressive failure analysis of composite laminates containing a central hole. It was shown that the proposed plastic damage model provided the sufficient accuracy in the prediction of failure loads or failure stresses.

Table 1: Material properties of AS4/PEEK and model parameters

E_1^0	E_2^0	G_{12}^0	ν_{12}^0	X_t	X_c
127.6GPa	10.3GPa	6.0GPa	0.32	2023MPa	1234MPa
Y_t	Y_c	S_c	$G_{1t,c}$	$G_{1c,c}$	$G_{2t,c}$
92.7 MPa	176.0 MPa	82.6 MPa	128.0 N/mm	128.0 N/mm	5.6 N/mm
$G_{2c,c}$	$G_{6,c}$	α	β	n	η
9.31 N/mm	4.93 N/mm	1.5	295.0274	0.142857	0.0002

Table 2: Comparison of the failure loads between experimental data and the FE analyses of AS4/PEEK $[0/45/90/\text{-}45]_{2s}$ composit laminates.

D(mm)	Failure load (kN)				Error %		
	Test	Present	Model 1	Model 2	Present	Model 1	Model 2
2	22.98	21.65	19.94	21.69	-5.792	-15.246	-5.614
3	19.31	18.12	13.63	17.65	-6.151	-41.673	-8.597
5	15.31	16.43	12.00	15.34	7.325	-27.583	0.196
8	11.67	13.11	10.06	12.46	12.296	-16.004	6.769
10	9.22	10.58	8.67	10.77	14.768	-6.344	16.811

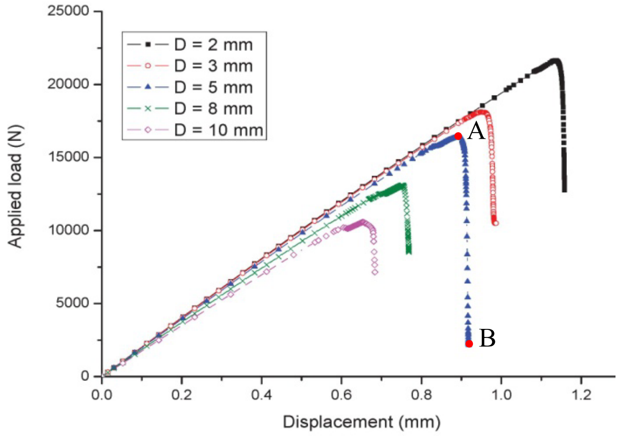

Figure 1: Predicted load vs displacement curves of AS4/PEEK $[0/45/90/\text{-}45]_{2s}$ laminates.

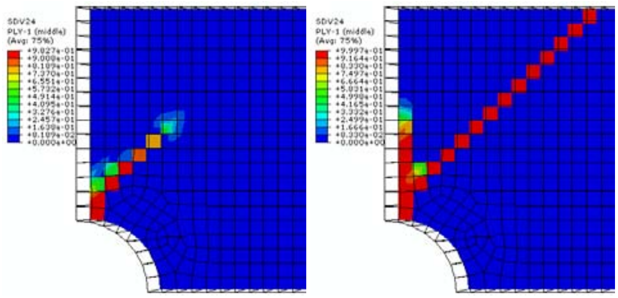

(a) $d_1$at A (b) $d_1$at B

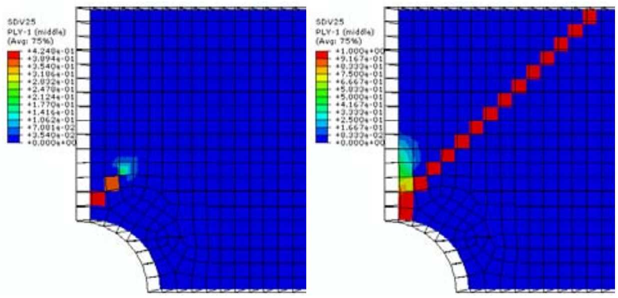

(c) d_2 at A (d) d_2 at B

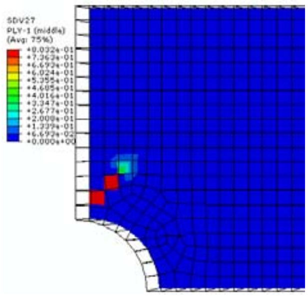

(e) d_6 at A

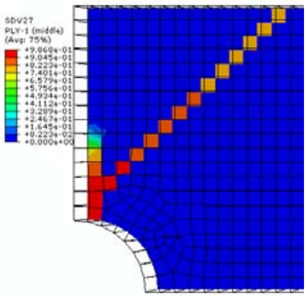

(f) d_6 at B

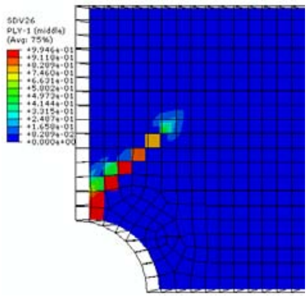

(g) d_3 at A

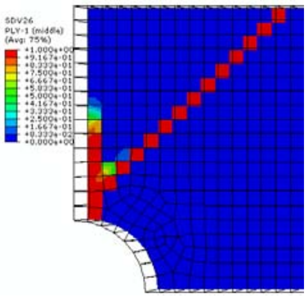

(h) d_3 at B

Figure 2: Evolution of damage in 0 ° ply of [0/45/90/ -45]2s laminate.

References

[1] P. Ladeveze and E. Le Dantec. “Damage modelling of the elementary ply for laminated composites”. *Composites Science and Technology*, Vol. 43, No. 3, pp 257-267, 1992.

[2] A. Matzenmiller, J. Lubliner and R. L. Taylor. “A constitutive model for anisotropic damage in fiber-composites”. *Mechanics of Materials*, Vol. 20, No. 2, pp125-152, 1995

[3] P. Maimí, P. P. Camanho, J. A. Mayugo and C. G. Davila. “A continuum damage model for composite laminates: Part I – Constitutive model”. *Mechanics of Materials*, Vol. 39, No. 10, pp 897-908, 2007.

[4] P. Maimí, P. P. Camanho, J. A. Mayugo and C. G. Davila. “A continuum damage model for composite laminates: Part II – Computational implementation and validation”. *Mechanics of Materials*, Vol. 39, No. 10, pp 909-919, 2007.

[5] I. Lapczyk and J. A. Hurtado. “Progressive damage modeling in fiber-reinforced materials”. *Composites Part A: Applied Science and Manufacturing*, Vol. 38, No. 11, pp 2333-2341, 2007.

[6] F. P. Van Der Meer and L. J. Sluys. “Continuum models for the analysis of progressive failure in composite laminates”. *Journal of Composite Materials*, Vol. 43, No. 20, pp 2131-2156, 2009.

[7] W. Van Paepegem, I. De Baere, and J. Degrieck. “Modelling the nonlinear shear stress-strain response of glass fibre-reinforced composites. Part I: Experimental results”. *Composites Science and Technology*, Vol. 66, No. 10, pp 1455-1464, 2006.

[8] M. C. Lafarie-Frenot and F. Touchard. “Comparative in-plane shear behaviour of long-carbon-fibre composites with thermoset and thermoplastic matrix”. *Composites Science and Technology*, Vol. 52, No. 3, pp 417-425, 1994.

[9] X. Xiao. “Modeling energy absorption with a damage mechanics based composite material model”. *Journal of composite materials,* Vol. 43, No. 5, pp 427-444, 2009.

[10] R. Maa and J. Cheng. “A CDM-based failure model for predicting strength of notched composite laminates”. *Composites Part B: Engineering*, Vol. 33, No. 6, pp 479-489, 2002.

[11] C. T. Sun and J. L. Chen. “A simple flow rule for characterizing nonlinear behavior of fiber composites”. *Journal of Composite Materials*, Vol. 23, No. 10, pp 1009-1020, 1989.

[12] Z. Hashin. “Failure criteria for unidirectional fiber composites”. *Journal of Applied Mechanics-T ASME,* Vol. 47, No. 2, pp 329-334, 1980.

[13] V. M. Winn and S. Sridharan. “An investigation into the accuracy of a one-parameter nonlinear model for unidirectional composites”. *Journal of Composite Materials*, Vol. 35, No. 16, pp 1491-1507, 2001.

[14] R. Faria, J. Oliver and M. Cervera. “A strain-based plastic viscous-damage model for massive concrete structures”. *International Journal of Solids and Structures*, Vol. 35, No. 14, pp 1533-1558, 1998.

[15] Z. Bazant and B. Oh. “Crack band theory for fracture of concrete”. *Materials and Structures*, Vol. 16, pp 155-177, 1983.

[16] S. T. Pinho. *Modelling failure of laminated composites using physically-based failure models*. Phd thesis. Department of Aeronautics, Imperial College, London, UK. 2005.

[17] C. T. Sun and K. J. Yoon. “Elastic-plastic analysis of AS4/PEEK composite laminate using a one-parameter plasticity model”. *Journal of Composite Materials*, Vol. 26, No. 2, pp 293-308, 1992.

[18] C. T. Sun and Y. Rui. “Orthotropic elasto-plastic behavior of AS4/PEEK thermoplastic composite in compression”. *Mechanics of Materials*, Vol. 10, No. 1-2, pp 117-125, 1990.

[19] M.Kawai, Y. Masuko, Y. Kawase, and R. Negishi. “Micromechanical analysis of the off-axis rate-dependent inelastic behavior of unidirectional AS4/PEEK at high temperature”. *International Journal of Mechanical Science*, Vol. 43, No. 9, pp 2069-2090, 2001.

[20] D. R. Carlie, D. C. Leach, D. R. Moore, and N. Zahlan. “Mechanical properties of the carbon fiber/PEEK APC-2/AS-4 for structural applications”. *Advances in thermoplastic matrix composite materials*, pp 199-212, 1989.

[21] S. L. Donaldson. “Fracture toughness testing of graphite/epoxy and graphite/PEEK composites”. *Composites*, Vol. 16, No. 2, pp 103-112, 1985.